



CHORUS

This is the accepted manuscript made available via CHORUS. The article has been published as:

Nuclear transparency of the charged hadrons produced in the electronuclear reaction

Swapn Das

Phys. Rev. C **105**, 035204 — Published 25 March 2022

DOI: [10.1103/PhysRevC.105.035204](https://doi.org/10.1103/PhysRevC.105.035204)

Nuclear transparency of the charged hadrons produced in the electronuclear reaction

Swapam Das ¹

*Nuclear Physics Division, Bhabha Atomic Research Centre,
Trombay, Mumbai 400085, India*

Homi Bhabha National Institute, Anushakti Nagar, Mumbai 400094, India

Abstract

The nuclear transparency of the charged hadrons produced in the (e, e') reaction on nuclei has been calculated using Glauber model for the nuclear reaction. The color transparency (CT) of produced hadrons and the short-range correlation (SRC) of nucleons in the nucleus have been incorporated in Glauber model to investigate their effects on the nuclear transparency. The calculated results for the proton and pion are compared with the data.

1 Introduction

The hadron-nucleus cross section is less than that in the plane wave impulse approximation (PWIA) because the initial and(or) final state interaction(s) of a hadron with the nucleus are neglected in PWIA. This phenomenon is characterized by the nuclear transparency T_A , defined [1] as

$$T_A = \frac{\sigma_{hA}}{\sigma_{hA(PWIA)}}, \quad (1)$$

where σ_{hA} represents the hadron-nucleus cross section.

The transverse size d_{\perp} of the hadron produced in a nucleus due to the space-like high momentum transfer Q^2 is reduced as $d_{\perp} \sim 1/Q$ [1, 2]. The reduced (in size) hadron is referred as point like configuration (PLC) [1]. According to Quantum Chromodynamics, a color neutral PLC has reduced interaction with the nucleon in a nucleus because the sum of its gluon emission amplitudes cancel [1, 3]. The PLC expands to the size of physical hadron, as it moves up to a length (~ 1 fm) called hadron formation length l_h [1, 4]:

$$l_h = \frac{2k_h}{\Delta M^2}, \quad (2)$$

where k_h is the momentum of hadron in the laboratory frame. ΔM^2 is related to the mass difference between the hadronic states originating due to the (anti)quarks fluctuation in PLC. The interaction of PLC with the nucleon in a nucleus increases, as its size enlarges

¹email: swapand@barc.gov.in

during its passage through the nucleus. The decrease in the hadron-nucleon cross section in a nucleus, as explained by Glauber model [5], leads to the increase in the hadron-nucleus cross section. Therefore, the transparency T_A in Eq. (1) of the hadron raises. The enhancement in T_A due to the above phenomenon is referred as color transparency (CT) of the hadron. The physics of CT for hadrons have been discussed elaborately in Refs. [3, 6].

The experiments on the nuclear transparency in the $A(p, pp)$ reactions had been done at Brookhaven National Laboratory (BNL) [7] to search the CT of proton (p CT). The measured spectra for nuclei show a peak in the energy distribution that could not be reproduced by the results calculated considering the p CT in Glauber model [8]. The data can be understood by other mechanisms (e.g., see Brodsky et al. [9] and Ralston et al. [10]) for the pp scattering in a nucleus. The p CT is not also seen in the $A(e, e'p)$ experiment done at Stanford Linear Accelerator Center (SLAC) [11] and Jefferson Laboratory (JLab) [12] for the photon virtuality $Q^2 = 0.64 - 8.1 \text{ GeV}^2$. The transparency measured in the $(e, e'p)$ reaction on ^{12}C for $8 \leq Q^2(\text{GeV}^2) \leq 14.2$ [13] at the upgraded JLab facility agrees with the previous observations [11, 12]. The calculated proton transparency in this reaction [14, 15]) corroborates the experimental finding.

Since the meson is a bound state of two quarks (i.e., quark-antiquark) the PLC formation of it can be more probable than that of the baryon, a three quarks (qqq) system. The color transparency is unambiguously reported from Fermi National Accelerator Laboratory (FNAL) [16] in the experiment of the nuclear diffractive dissociation of pion (of $500 \text{ GeV}/c$) to dijets. The color transparency is also illustrated in the π^- meson photoproduction [17] and ρ^0 meson electroproduction (from nuclei) experiments [18]. There exist calculated results for the ρ -meson color transparency in the energy region available at JLab [1, 19].

The nuclear transparency of the π^+ meson produced in the $A(e, e')$ process was measured at JLab for $Q^2 = 1.1 - 4.7 \text{ GeV}^2$ [20]. The data have been understood by the pionic color transparency (π CT) [4]. Larson et al., [21] described the momentum dependence of π CT in the above reaction. The π CT in the electronuclear reaction has also been studied by Cosyn et al., [22] and Kaskulov et al., [23] for the energy region available at JLab [20]. Larionov et al., [4] estimated the π CT in the (π^-, l^+l^-) reaction on nuclei for $p_\pi = 5 - 20 \text{ GeV}/c$, which can be measured at the forth-coming facilities in Japan Proton Accelerator Research Complex (J-PARC) [24]. This reaction provides informations complementary to those obtained from the $A(\gamma^*, \pi)$ reaction. Miller and Strikman [25] illustrated large CT in the pionic knockout of the proton off nuclei at the energy 200 GeV available at CERN COMPASS experiment.

The enhancement in T_A due to σ_{hA} in Eq. (1) can also occur because of the short-range correlation (SRC) of nucleon in the nucleus. The SRC arises because of the repulsive (short-range) interaction between the nucleons bound in a nucleus. This interaction keeps

the bound nucleons apart (~ 1 fm), which is called nuclear granularity [8]. Therefore, the SRC prevents the shadowing of the hadron-nucleon interaction due to the surrounding nucleons present in a nucleus. This occurrence, as elucidated by Glauber model [5], leads to the enhancement in σ_{hA} . The SRC is widely used to investigate various aspects in the nuclear physics [26].

2 Formalism

The hadron h is produced in the $A(e, e')X$ reaction because of the interaction of the virtual photon γ^* (emitted at the ee' vertex) with the nucleus A . In this reaction, the nucleus in the final state denoted by X is unspecified. The scattering amplitude for the $\gamma^*A \rightarrow hX$ transition, according to Glauber model [1], can be written as

$$F_{X0}[(\mathbf{q} - \mathbf{k}_h)_\perp] = \frac{iq}{2\pi} \int d\mathbf{b} e^{i(\mathbf{q} - \mathbf{k}_h)_\perp \cdot \mathbf{b}} \Gamma_{X0}^{\gamma^*h}(\mathbf{b}), \quad (3)$$

where \mathbf{q} and \mathbf{k}_h are the momenta of γ^* and h respectively. $\Gamma_{X0}^{\gamma^*h}(\mathbf{b})$ describes the matrix element for the transition of the nucleus from its initial to final states, i.e.,

$$\Gamma_{X0}^{\gamma^*h}(\mathbf{b}) = \langle X | \Gamma_A^{\gamma^*h}(\mathbf{b}, \mathbf{r}_1, \dots, \mathbf{r}_A) | 0 \rangle, \quad (4)$$

where $|0\rangle$ denotes the ground state of the target nucleus and $|X\rangle$ represents the unspecified nuclear state in the exit channel. The nuclear profile operator $\Gamma_A^{\gamma^*h}(\mathbf{b}, \mathbf{r}_1, \dots, \mathbf{r}_A)$ [1, 27] is given by

$$\Gamma_A^{\gamma^*h}(\mathbf{b}, \mathbf{r}_1, \dots, \mathbf{r}_A) = \sum_i \Gamma^{\gamma^*h}(\mathbf{b} - \mathbf{b}_i) e^{i(\mathbf{q} - \mathbf{k}_h)_\parallel z_i} \prod_{j \neq i}^{A-1} [1 - \Gamma^{hN}(\mathbf{b} - \mathbf{b}_j) \theta(z_j - z_i)]. \quad (5)$$

The summation i is taken over the number of nucleons in the nucleus participated for the hadron production, e.g., the protons in the nucleus take part to produced charged hadron in the reaction.

$\Gamma^{\gamma^*h}(\tilde{\mathbf{b}})$ is the two-body profile function for the hadron produced from the nucleon, i.e., $\gamma^*N \rightarrow hN$ process. It is related to the reaction amplitude $f_{\gamma^*h}(\tilde{\mathbf{q}}_\perp)$ [1] as

$$\Gamma^{\gamma^*h}(\tilde{\mathbf{b}}) = \frac{1}{i2\pi q} \int d\tilde{\mathbf{q}}_\perp e^{-i\tilde{\mathbf{q}}_\perp \cdot \tilde{\mathbf{b}}} f_{\gamma^*h}(\tilde{\mathbf{q}}_\perp). \quad (6)$$

The two-body profile function $\Gamma^{hN}(\tilde{\mathbf{b}})$ is connected to hN (hadron-nucleon) elastic scattering amplitude $f_{hN}(\tilde{\mathbf{q}}_\perp)$ [1, 5] as

$$f_{hN}(\tilde{\mathbf{q}}'_\perp) = \frac{ik_h}{2\pi} \int d\tilde{\mathbf{b}}' e^{i\tilde{\mathbf{q}}'_\perp \cdot \tilde{\mathbf{b}}'} \Gamma^{hN}(\tilde{\mathbf{b}}'). \quad (7)$$

The nuclear states, assuming the independent particle model [28], can be written in terms of the single particle state Φ as $|0\rangle = \prod_{l=1}^A |\Phi_0(\mathbf{r}_l)\rangle$ and $|X\rangle = |\Phi_X(\mathbf{r}_m)\rangle \prod_{n \neq m}^{A-1} |\Phi_0(\mathbf{r}_n)\rangle$. Using those, $\Gamma_{X0}^{\gamma^*h}(\mathbf{b})$ in Eq. (4) can be written as

$$\Gamma_{X0}^{\gamma^*h}(\mathbf{b}) = \sum_i \int d\mathbf{r}_i \Phi_X^*(\mathbf{r}_i) \Gamma^{\gamma^*h}(\mathbf{b} - \mathbf{b}_i) e^{i(\mathbf{q} - \mathbf{k}_h)_\parallel z_i} \Phi_0(\mathbf{r}_i) D(\mathbf{b}, z_i), \quad (8)$$

where $D(\mathbf{b}, z_i)$ is given by

$$\begin{aligned} D(\mathbf{b}, z_i) &= \prod_{j \neq i}^{A-1} \int d\mathbf{r}_j \Phi_0^*(\mathbf{r}_j) [1 - \Gamma^{hN}(\mathbf{b} - \mathbf{b}_j) \theta(z_j - z_i)] \Phi_0(\mathbf{r}_j) \\ &= \left[1 - \frac{1}{A} \int d\mathbf{b}_j \Gamma^{hN}(\mathbf{b} - \mathbf{b}_j) \int dz_j \theta(z_j - z_i) \varrho(\mathbf{r}_j) \right]^{A-1}. \end{aligned} \quad (9)$$

$\varrho(\mathbf{r}_j)$ in above equation is the matter density distribution of the nucleus, i.e., $\varrho(\mathbf{r}_j) = A |\Phi_0(\mathbf{r}_j)|^2$. $\varrho(\mathbf{b}_j, z_j)$ can be replaced by $\varrho(\mathbf{b}, z_j)$ since $\Gamma^{hN}(\mathbf{b} - \mathbf{b}_j)$ varies much rapidly than $\varrho(\mathbf{b}_j, z_j)$ [1]. Using Eq. (7) and $\mathcal{L}t_{n \rightarrow \infty} (1 + \frac{x}{n})^n = e^x$, the above equation can be simplified to

$$D(\mathbf{b}, z_i) \simeq e^{-\frac{1}{2} \sigma_t^{hN} [1 - i\alpha_{hN}] T(\mathbf{b}, z_i)}, \quad (10)$$

where α_{hN} denotes the ratio of the real to imaginary part of the hadron-nucleon scattering amplitude $f_{hN}(0)$, and $\sigma_t^{hN} = \frac{4\pi}{k_h} \text{Im}[f_{hN}(0)]$ is the hadron-nucleon total cross section. $T(\mathbf{b}, z_i)$ is the partial thickness function of the nucleus, i.e.,

$$T(\mathbf{b}, z_i) = \int_{z_i}^{\infty} dz_j \varrho(\mathbf{b}, z_j). \quad (11)$$

Using Eq. (8), $F_{X0}[(\mathbf{q} - \mathbf{k}_h)_\perp]$ in Eq. (3) can be expressed as

$$\begin{aligned} F_{X0} &= \frac{iq}{2\pi} \int d\mathbf{b} e^{i(\mathbf{q} - \mathbf{k}_h)_\perp \cdot \mathbf{b}} \sum_i \int d\mathbf{r}_i \Phi_X^*(\mathbf{r}_i) \Gamma^{\gamma^*h}(\mathbf{b} - \mathbf{b}_i) e^{i(\mathbf{q} - \mathbf{k}_h)_\parallel z_i} \Phi_0(\mathbf{r}_i) D(\mathbf{b}, z_i), \\ &= \sum_i \int d\mathbf{r}_i \Phi_X^*(\mathbf{r}_i) f_{hN}^{(i)}([\mathbf{q} - \mathbf{k}_h]_\perp) e^{i(\mathbf{q} - \mathbf{k}_h)_\parallel \mathbf{r}_i} \Phi_0(\mathbf{r}_i) D(\mathbf{r}_i), \end{aligned} \quad (12)$$

where $f_{hN}^{(i)}$, defined in Eq. (7), can be considered identically equal for all nucleons.

3 Result and Discussions

The nuclear transparency T_A of the hadron produced in the $A(e, e')X$ reaction has been calculated to describe its dependence on the photon virtuality Q^2 in the multi-GeV region. The nucleus in the final state $|X\rangle$ differs from its initial state $|0\rangle$ (i.e., ground state)

for the charged hadron production, i.e., $\Phi_X \neq \Phi_0$ and $F_{00} = 0$. To calculate the cross section, $|F_{X0}|^2$ is to multiply by the phase-space of the reaction and that is to divide by the incident flux. Since the final state $|X\rangle$ of the nucleus is not detected, the summation over all states X has to carry out. In the multi-GeV region, the phase space of the reaction can be considered independent of the state X , and therefore, the nuclear transparency T_A can be written [1] as

$$T_A = \frac{\sum_{X \neq 0} |F_{X0}|^2}{\sum_{X \neq 0} |F_{X0}|_{PWIA}^2}. \quad (13)$$

The hadron-nucleon cross section σ_t^{hN} in the free-space is used in Eq. (10) to evaluate T_A in Glauber model. To look for the color transparency (CT), σ_t^{hN} (according to quantum diffusion model [2, 21]) has to replace by $\sigma_{t,CT}^{hN}$:

$$\sigma_{t,CT}^{hN}(Q^2, l_z) = \sigma_t^{hN} \left[\left\{ \frac{l_z}{l_h} + \frac{n_q^2 \langle k_t^2 \rangle}{Q^2} \left(1 - \frac{l_z}{l_h} \right) \right\} \theta(l_h - l_z) + \theta(l_z - l_h) \right], \quad (14)$$

where Q^2 is the space-like four-momentum transfer, i.e., photon virtuality. n_q denotes the number of valence quak-(anti)quark present in the hadron, e.g., $n_q = 2(3)$ for pion (proton) [2]. k_t illustrates the transverse momentum of the (anti)quark: $\langle k_t^2 \rangle^{1/2} = 0.35$ GeV/ c . l_z is the path length traversed by the hadron after its production. The hadron formation length $l_h (\propto \frac{1}{\Delta M^2})$ is already defined in Eq. (2).

The short-range correlation (SRC) can be incorporated by replacing the nuclear density distribution ϱ in Eq. (11) by

$$\varrho(\mathbf{b}, z_j) \rightarrow \varrho(\mathbf{b}, z_j) C(|z_j - z_i|), \quad (15)$$

where $C(u)$ represents the correlation function [8]. Using the nuclear matter estimate, it can be written as

$$C(u) = \left[1 - \frac{h(u)^2}{4} \right]^{1/2} [1 + f(u)], \quad (16)$$

with $h(u) = 3 \frac{j_1(k_F u)}{k_F u}$ and $f(u) = -e^{-\alpha u^2} (1 - \beta u^2)$. The Fermi momentum k_F is chosen equal to 1.36 fm^{-1} . $C(u)$ with the parameters $\alpha = 1.1 \text{ fm}^{-2}$ and $\beta = 0.68 \text{ fm}^{-2}$ agrees well that derived from the many-body calculations [8].

The nuclear transparency T_A of the charged hadron, i.e., proton and π^+ meson, produced in the semi-inclusive electronuclear reaction has been calculated using Glauber model (GM), where the measured nuclear density distribution $\varrho(r)$ [29], and hadron-nucleon cross section σ_t^{hN} [30] are used. As shown later, the calculated results due to GM (presented by the medium-dashed curves) underestimate the measured T_A for both proton and pion. Therefore, GM has been modified by taking account of the CT and SRC. The dot-dot-dashed and dot-dashed curves denote the calculated T_A due to the incorporation

of the CT in GM for ΔM^2 , defined in Eq. (2), taken equal to 0.7 and 1.4 GeV² respectively. The calculated results increases with Q^2 because the CT depends on the energy. T_A evaluated due to the SRC included in GM are presented by the solid curves. They do not show Q^2 dependence since the SRC (unlike CT) is independent of energy.

The proton transparency $T_A(p)$ in the $A(e, e'p)X$ reaction has been calculated using the CT of proton (p CT) in Glauber model (GM+ p CT) for ¹²C, ⁵⁶Fe and ¹⁹⁷Au nuclei. The calculated results vs Q^2 are compared in Fig. 1 with the data reported from SLAC [11] (white squares) and JLab [12, 13] (black circles). Fig. 1(a) shows the CT does not exist for the proton moving through ¹²C for a wide range of Q^2 , i.e., 0.64 – 14.2 GeV². This is corroborated by the results for other nuclei shown in Figs. 1(b) and (c), where the data are available for lesser range of Q^2 , i.e., $0.64 \leq Q^2 \leq 8.1$ GeV² for ⁵⁶Fe and $0.64 \leq Q^2 \leq 6.77$ GeV² for ¹⁹⁷Au. Fig. 1 also shows the calculated $T_A(p)$ due to the inclusion of the SRC in Glauber model (GM+SRC) reproduce the data reasonably well for all nuclei.

There exist calculations where the p CT is not considered to evaluate $T_A(p)$ in the $A(e, e'p)X$ reaction. For example, Frankel et al. [14] have calculated $T_A(p)$ using Glauber Monte Carlo method (GMCM) in which Jastrow-type spatial correlation is included. The density of the C, Fe and Au nuclei is described by Woods-Saxon (WS) single-particle density. They have also calculated $T_A(p)$, only for ¹²C nucleus, using the nuclear density accounted by filled $0s_{1/2}$ - $0p_{3/2}$ shell-model (SM) wave functions. The calculated results are shown in Fig. 2, where the long-dashed curves arise due to GMCM+WS and the short-dashed curves occur because of GMCM+SM. Lava et al. [15] have shown $T_A(p)$ evaluated using the relativistic distorted-wave impulse approximation (RDWIA) and relativistic multiple-scattering Glauber approximation (RMSGGA). The final-state interaction treated in those approaches differs from each-other. As mentioned in Ref. [15], the SRC of nucleon has been let out and the calculated $T_A(p)$ for ²⁰⁸Pb is compared to ¹⁹⁷Au data. The results due to RDWIA (short-dashed curves) and RMSGGA (long-dashed curves) are presented in Fig. 3. The above mentioned calculated results are compared with $T_A(p)$ due to GM+SRC (solid curves in Figs. 2 and 3) in the present work, as explained in Fig. 1. The data are taken from Refs. [11, 12, 13].

The pionic transparency $T_A(\pi^+)$ for $Q^2 = 1.1 - 4.69$ GeV² in the $A(e, e'\pi^+)X$ reaction was measured at JLab [20] for ¹²C, ²⁷Al, ⁶³Cu and ¹⁹⁷Au nuclei to search the color transparency of pion (π CT). The data for all nuclei (except ¹²C) show the enhancement of $T_A(\pi^+)$ with Q^2 . Proposals are there to measure $T_A(\pi^+)$ at JLab for higher Q^2 , i.e., $5 \leq Q^2 \leq 9.5$ GeV² [3, 31]. Therefore, $T_A(\pi^+)$ for $Q^2 = 1.1 - 9.5$ GeV² have been calculated and those are presented in Fig. 4 along with the data available from JLab [20]. The calculated results due to the π CT comprised in Glauber model (GM+ π CT) are accord with both the Q^2 dependence and magnitude of the data. $T_A(\pi^+)$ estimated incorporating the SRC in Glauber model (GM+SRC) do not describe the Q^2 dependence of the data

but those agree with large number of data points within the errors. Therefore, the data of $T_A(\pi^+)$ in the region of $Q^2 = 5 - 9.5 \text{ GeV}^2$ are necessary to prove the existence of πCT .

The effects of πCT (for $\Delta M^2 = 0.7 \text{ GeV}^2$) and SRC (Jastrow-type) on $T_A(\pi^+)$ in the $A(e, e'\pi^+)X$ reaction have also been discussed by Cosyn et al. [22] in their calculation based on the relativistic multiple-scattering Glauber approximation (RMSGGA). In Fig. 5, the calculated results due to RMSGGA+ πCT and RMSGGA+SRC are denoted by the long-dashed and short-dashed curves respectively. Kaskulov et al. [23] have studied $T_A(\pi^+)$ in the above reaction using the couple-channel (CC) treatment for the pion-nucleon interaction, and discussed the effects of pion production mechanisms in the elementary (γ^*, π^+) reaction. However, they have not considered the SRC of nucleon. Amongst the calculated results [23], $T_A(\pi^+)$ evaluated using Lund model (LM) for the pion formation time (dilatated) along with the pedestal value of the pion-nucleon effective cross-section (Q^2 independent) provides good description of the data. The calculated results due to CC+LM are denoted by the long-dashed curves in Fig. 6. Other curves in Figs. 5 and 6 occurred due to present work (see Fig. 4) are shown for comparison. The data are taken from Ref. [20].

4 Conclusions

The nuclear transparencies T_A of the proton and π^+ meson produced in the (e, e') reaction on nuclei have been calculated using Glauber model for the wide range of photon virtuality Q^2 . T_A estimated using Glauber model do not reproduce the measured transparencies for both proton and pion. To realize the data, T_A is calculated incorporating the color transparency of the produced hadron and the short-range correlation of the bound nucleon in Glauber model. The calculated results for the proton and pion are compared with the data. The transparency of proton $T_A(p)$ evaluated using the color transparency in Glauber model does not reproduce the data, where as the calculated $T_A(p)$ due to the short-range correlation added in Glauber model is well accord with the data. The calculated transparency of pion $T_A(\pi^+)$ considering the color transparency in Glauber model agrees with both the Q^2 dependence and magnitude of the data, available for $1.1 \leq Q^2 \leq 4.69 \text{ GeV}^2$. The calculated $T_A(\pi^+)$ due to the inclusion of the short-range correlation in Glauber model agree with large number of data points within the errors, but those do not explain the Q^2 dependence of the measured spectra. Therefore, $T_A(\pi^+)$ for $Q^2 = 5 - 9.5 \text{ GeV}^2$ to be measured at JLab are required to confirm the pionic color transparency.

5 Acknowledgement

The author appreciates the anonymous referee for the comments which improve the quality of the work. The author is grateful to Dipangkar Dutta for the discussions on experimental results, and thanks A. K. Gupta and S. M. Yusuf for their encouragement to work on theoretical nuclear physics.

References

- [1] G. T. Howell and G. A. Miller, *Phys. Rev. C* **88** (2013) 035202.
- [2] G. R. Farrar, H. Liu, L. L. Frankfurt and M. I. Strikman, *Phys. Rev. Lett.* **61** (1988) 686.
- [3] D. Dutta, K. Hafidi, and M. Strikman, *Prog. Part. Nucl. Phys.* **69** (2013) 1.
- [4] A. B. Larionov, M. Strikman and M. Bleicher, *Phys. Rev. C* **93** (2016) 034618.
- [5] R. J. Glauber, in *Lectures in Theoretical Physics*, edited by W. E. Brittin et al. (Interscience, New York, 1959), Vol. I, p. 315; J. M. Eisenberg and D. S. Kolton, *Theory of Meson Interaction with Nuclei* (John Wiley & Sons, New York, 1980) p. 158.
- [6] L. L. Frankfurt, G. A. Miller and M. Strikman, *Annu. Rev. Nucl. Part. Sci.* **44** (1994) 501; L. Frankfurt and M. Strikman, *Phys. Rep.* **160** (1988) 235; P. Jain, B. Pire and J. P. Ralston, *Phys. Rep.* **271** (1996) 67.
- [7] A. S. Carroll et al., *Phys. Rev. Lett.* **61** (1988) 1698; I. Mardor et al., *Phys. Rev. Lett.* **81** (1998) 5085; A. Leksanov et al., *Phys. Rev. Lett.* **87** (2001) 212301; J. Aclander et al., *Phys. Rev. C* **70** (2004) 015208.
- [8] T.-S. H. Lee and G. A. Miller, *Phys. Rev. C* **45** (1992) 1863.
- [9] S. J. Brodsky and G. F. de Teramond, *Phys. Rev. Lett.* **60** (1988) 1924.
- [10] J. P. Ralston and B. Pire, *Phys. Rev. Lett.* **61** (1988) 1823.
- [11] T. G. O'Neill et al., *Phys. Lett. B* **351** (1995) 87; N. C. R. Makins et al., *Phys. Rev. Lett.* **72** (1994) 1986.
- [12] D. Dutta et al., *Phys. Rev. C* **68** (2003) 064603; D. Abbott et al., *Phys. Rev. Lett.* **80** (1998) 5072; K. Garrow et al., *Phys. Rev. C* **66** (2002) 044613.

- [13] D. Bhetuwal et al., Phys. Rev. Lett. **126** (2021) 082301.
- [14] S. Frankel, W. Frati and N. R. Walet, Phys. Rev. C **51** (1995) R1616.
- [15] P. Lava, M. C. Martínez, J. Rychebusch, J. A. Caballero and J. M. Udías, Phys. Lett. B **595** (2004) 177.
- [16] E. M. Aitala et al., Phys. Rev. Lett. **86** (2001) 4773.
- [17] D. Dutta et al. (E94104 Collaboration), Phys. Rev. C **68** (2003) 021001R.
- [18] A. Airapetian et al., Phys. Rev. Lett. **90** (2003) 052501; L. El Fassi et al., Phys. Lett. B **712** (2012) 326.
- [19] B. Z. Kopeliovich, J. Nemchik and I. Schmidt, Phys. Rev. C **76** (2007) 015205; L. Frankfurt, G. A. Miller and M. Strikman, Phys. Rev. C **78** (2008) 015208; K. Gallmeister, M. Kaskulov and U. Mosel, Phys. Rev. C **83** (2011) 015201.
- [20] B. Clasie et al., Phys. Rev. Lett. **99** (2007) 242502; X. Qian et al., Phys. Rev. C **81** (2010) 055209.
- [21] A. Larson, G. A. Miller and M. Strikman, Phys. Rev. C **74** (2006) 018201.
- [22] W. Cosyn, M. C. Martínez and J. Rychebusch, Phys. Rev. C **77** (2008) 034602.
- [23] M. M. Kaskulov, K. Gallmeister and U. Mosel, Phys. Rev. C **79** (2009) 015207.
- [24] S. Kumano, in 21st International Symposium on Spin Physics (SPIN 2014) Beijing, China, October 20-24, 2014: arXiv 1504.05264 [hep-ph]; Int. J. Mod. Phys. (Conference Series) **40** (2016) 1660009.
- [25] G. A. Miller and M. Strikman, Phys. Rev. C **82** (2010) 025205.
- [26] G. A. Miller and J. E. Spencer, Ann. Phys. (N.Y.) **100** (1976) 562; O. Benhar et al., Phys. Rev. C **44** (1991) 2328; S. Das, Phys. Scr. **96** (2021) 035304.
- [27] J. Hüfner, B. Kopeliovich and J. Nemchik, Phys. Lett. B **383** (1996) 362.
- [28] T. H. Bauer, R. D. Spital, D. R. Yennie and F. M. Pipkin, Rev. Mod. Phys. **50** (1978) 261; Erratum, **51** (1979) 407.
- [29] C. W. De Jager, H. De Vries and C. De Vries, At. Data and Nucl. Data Tables **14** (1974) 479; **36** (1987) 495.

- [30] P. A. Zyla et al., (Particle Data Group), Prog. Theor. Exp. **2020** (2020) 083C01; <https://pdg.lbl.gov/2020/hadronic-xsections/hadron.html>; C. Lechanoine-Leluc and F. Lehar, Rev. Mod. Phys. **65** (1993) 47; D. V. Bugg et al., Phys. Rev. **146** (1966) 980; S. Barshay, C. B. Dover and J. P. Vary, Phys. Rev. C **11** (1975) 360.
- [31] D. Dutta, private communication.

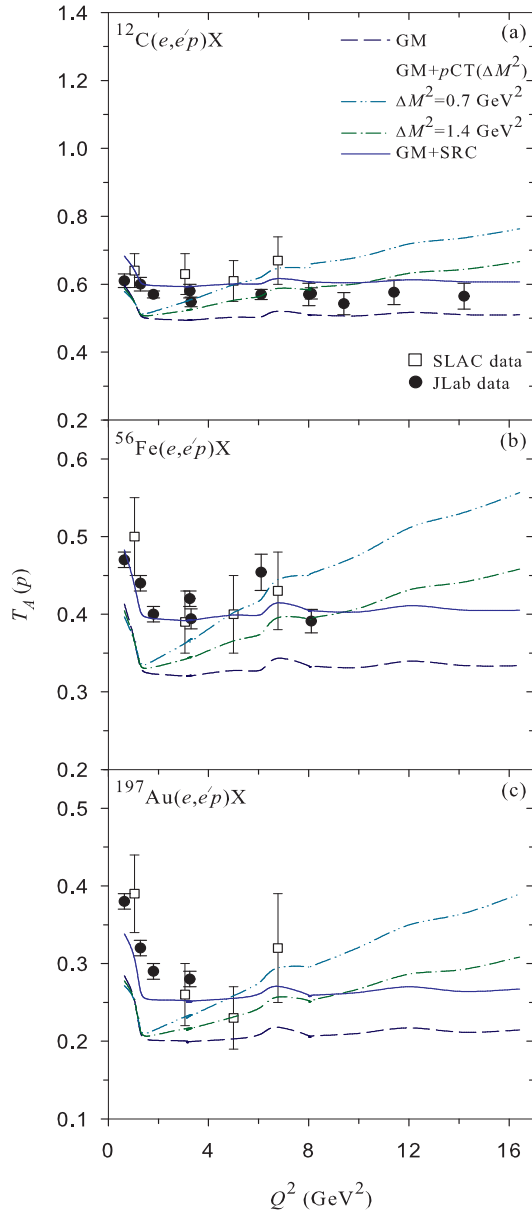


Figure 1: (color online). The calculated nuclear transparency of the proton $T_A(p)$ vs. photon virtuality Q^2 . The medium-dashed curves denote $T_A(p)$ evaluated using Glauber model (GM). The dot-dot-dashed and dot-dashed curves illustrate the proton color transparency (pCT) for two different values of ΔM^2 used in Glauber model (GM+ pCT), see text. The solid curves arise due to the inclusion of short-range correlation (SRC) in Glauber model (GM+SRC). The data are taken from Refs. [11, 12, 13].

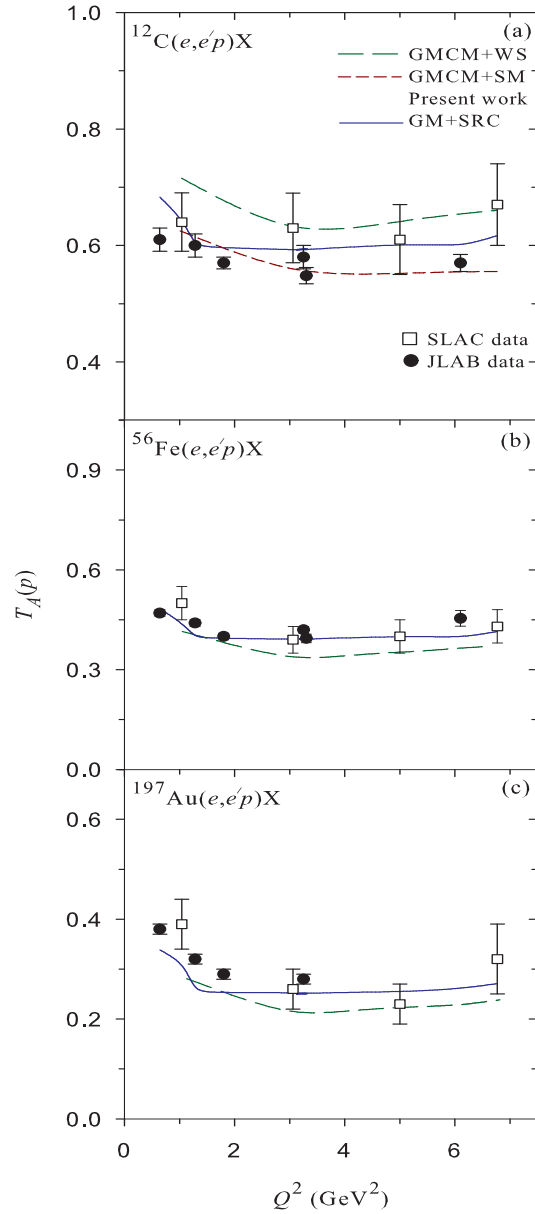


Figure 2: (color online). The proton transparency $T_A(p)$ calculated by Frankel et al. [14] using Glauber Monte Carlo method (GMCM). The density of nuclei is accounted by Woods-Saxon (WS) and that also is done by shell-model (SM) for ^{12}C only. The long-dashed and short-dashed curves arise because of GMCM+WS and GMCM+SM respectively. Those results are compared with $T_A(p)$ due to GM+SRC (solid curves) in the present work described in Fig. 1. The data are taken from Refs. [11, 12].

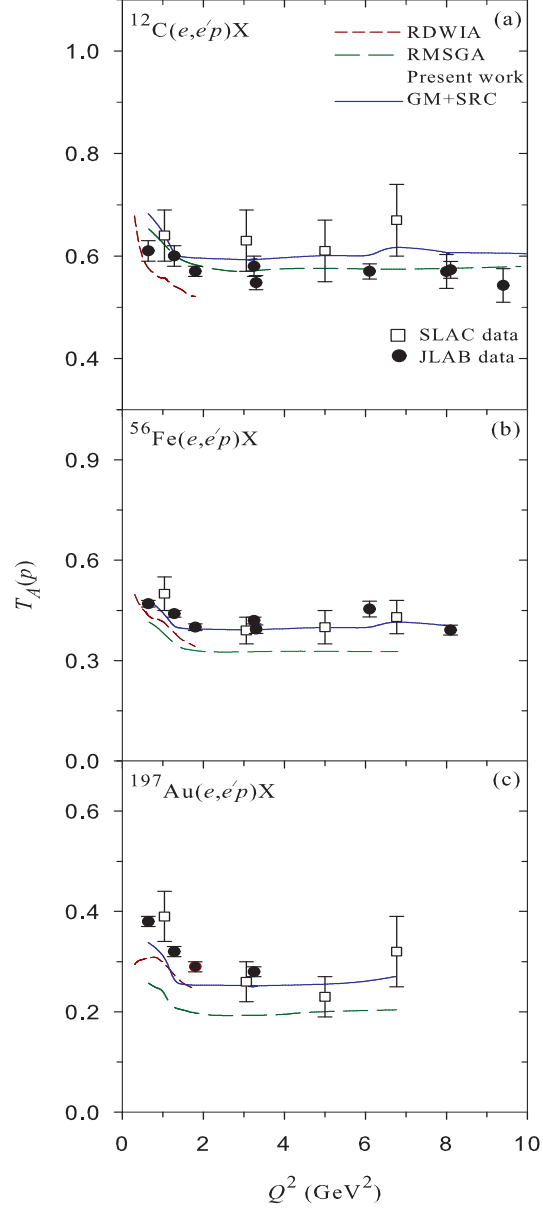


Figure 3: (color online). The short-dashed and long-dashed curves refer to the calculated proton transparency $T_A(p)$, as shown by Lava et al. [15], due to the relativistic distorted wave approximation (RDWIA) and relativistic multiple-scattering Glauber approximation (RMSGGA) respectively. The solid curves due to GM+SRC in the present work (as illustrated in Fig. 1) are shown for comparison. The data are taken from Refs. [11, 12, 13].

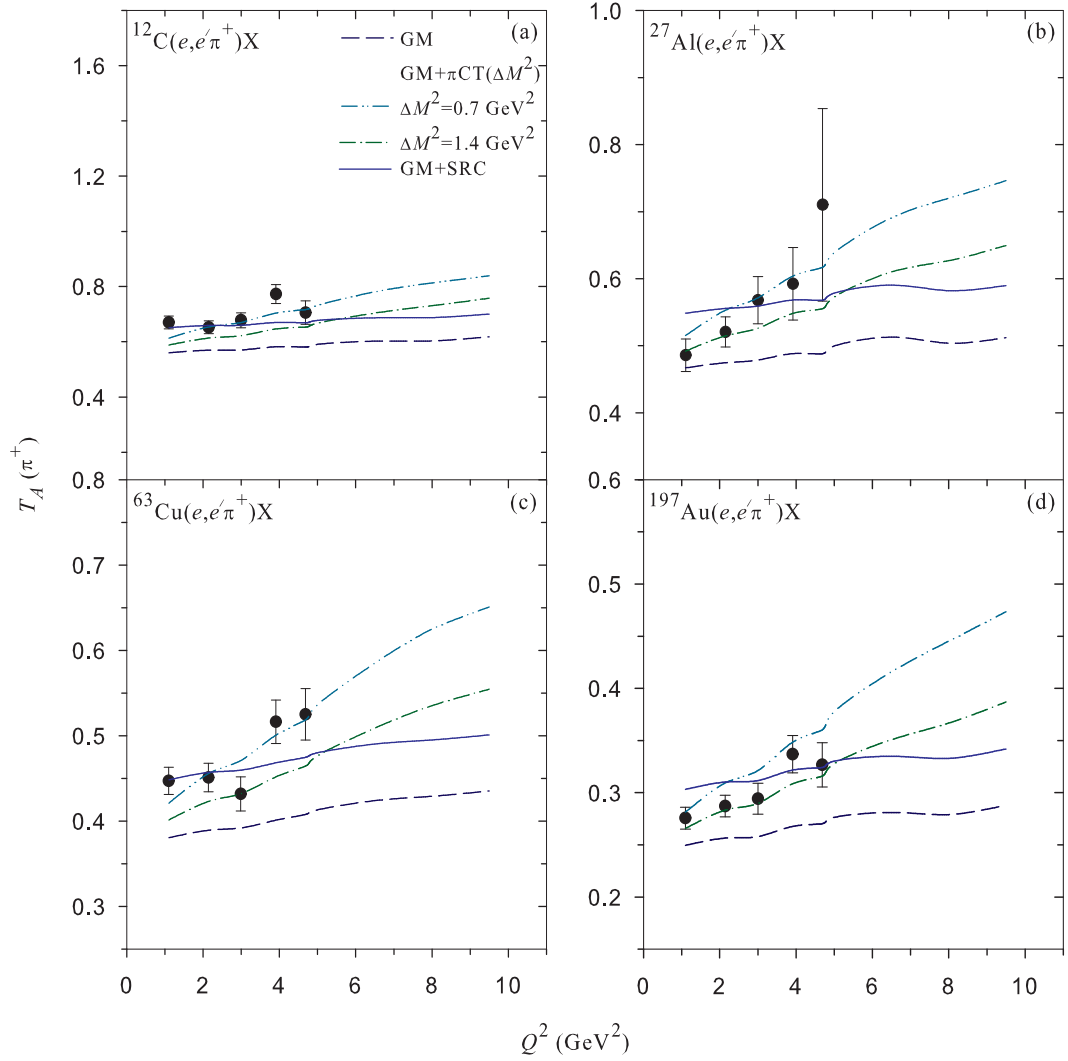


Figure 4: (color online). Same as those presented in Fig. 1 but for the pionic transparency $T_A(\pi^+)$. The data are taken from Ref. [20].

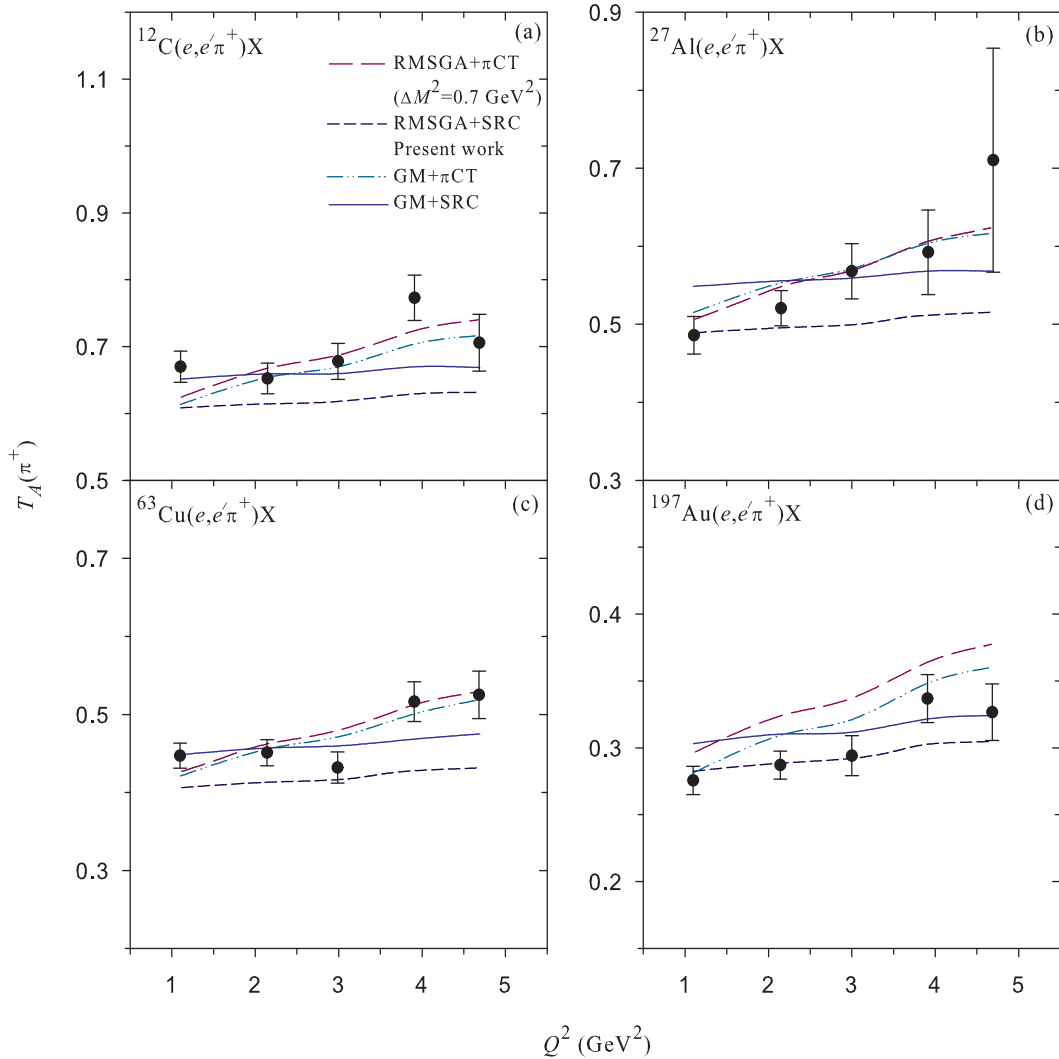


Figure 5: (color online). The pionic transparency $T_A(\pi^+)$ calculated by Cosyn et al., [22] using the relativistic multiple-scattering Glauber approach (RMSGGA). The effects of pionic color transparency (π CT) for $\Delta M^2=0.7$ GeV 2 and short-range correlation (SRC) comprised in RMSGGA are described by the long-dashed curves (RMSGGA+ π CT) and short-dashed curves (RMSGGA+SRC) respectively. Those results are compared with $T_A(\pi^+)$ due to GM+ π CT (dot-dot-dashed curves) and GM+SRC (solid curves) in the present work, see Fig. 4. The data are taken from Ref. [20].

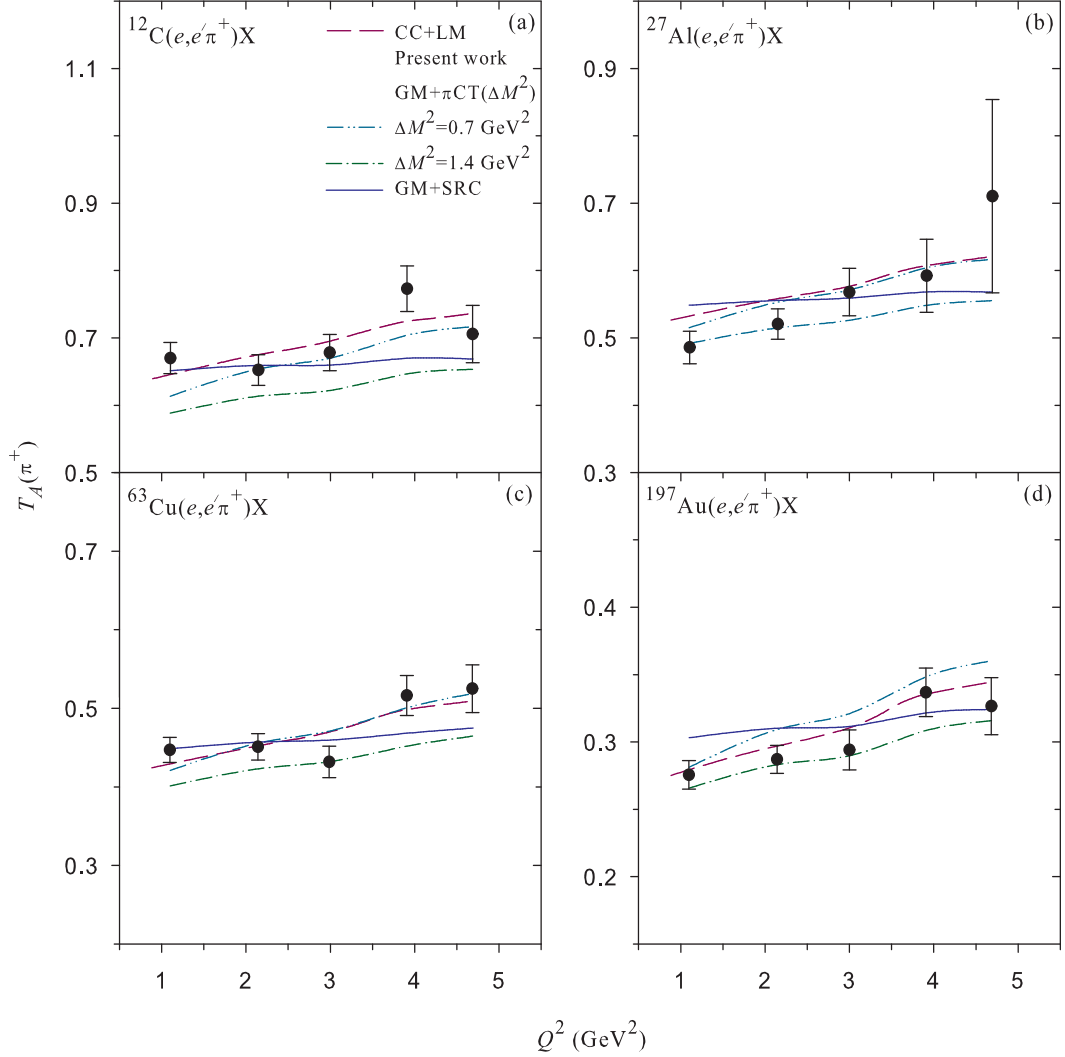


Figure 6: (color online). The transparency $T_A(\pi^+)$ calculated by Kaskulaov et al., [23] based on Lund model (LM) and couple-channel (CC) approach, see text. The long-dashed curves represent the calculated results due to CC+LM. Other curves occurred due to the present work (see Fig. 4) have been shown for comparison. The data are taken from Ref. [20].